

## EFFECT OF DEUTERIUM IMPLANTATION DOSE ON PROPERTIES OF CrN COATINGS

*A.S. Kuprin<sup>1</sup>, V.A. Belous<sup>1</sup>, O.M. Morozov<sup>1</sup>, V.D. Ovcharenko<sup>1</sup>, S.N. Dub<sup>2</sup>, G.N. Tolmachova<sup>1</sup>,  
E.N. Reshetnyak<sup>1</sup>, V.I. Zhurba<sup>1</sup>, V.O. Progolaieva<sup>1</sup>*

<sup>1</sup>*National Science Center “Kharkov Institute of Physics and Technology”, Kharkov, Ukraine;*

<sup>2</sup>*V.N. Bakul’ Institute of Superhard Materials, NAS of Ukraine, Kiev, Ukraine*

*E-mail: kuprin@kipt.kharkov.ua*

The methods of X-ray diffraction analysis, atomic-force microscopy, nanoindentation and thermodesorption spectroscopy have been applied to investigate the effect of a dose (from  $5 \cdot 10^{16}$  to  $1.5 \cdot 10^{18}$  D/cm<sup>2</sup>) of implanted deuterium with energy of 24 keV on the structure, surface morphology and mechanical properties of vacuum-arc CrN coatings. Deuterium ion implantation in the range of doses from  $5 \cdot 10^{16}$  to  $1.5 \cdot 10^{17}$  D/cm<sup>2</sup> decreases by 10...15% the nanohardness and elastic modulus of coatings. Under exposition to doses  $\geq 1 \cdot 10^{18}$  D/cm<sup>2</sup> the coating nanohardness sharply decreases because of blisters being formed and occupying about 30% of the CrN coating surface. Deuterium implantation did not lead to formation of new phases in the CrN coating.

### INTRODUCTION

Wide application of transition metal nitrides as protective coatings in industry is due to their excellent mechanical properties and high corrosion stability in aggressive environment. Vacuum-arc deposition makes it possible to obtain protective nitride films on different materials [1]. However, the use of such coatings in the atomic industry requires a comprehensive understanding of their behavior in the irradiation environments. At present, the extensive studies are carried out on stability of the properties of bulk nitrides [2] and nitride coatings [3–8] under different-type ion irradiations. Irradiation with inert gases creates radiation defects in the coating and can lead to amorphization and to blistering at high doses [9]. This negative factor can influence on the coating protective properties under radiation exposure. Nitride coatings have a higher radiation resistance, as compared to pure metals, steels and alloys, due to the perfect nanostructure and strong chemical bonds of elements. Chemically active gases, e. g. hydrogen and its isotopes, can initiate phase changes in materials leading to the degradation of their properties [10]. In water-cooled reactors, there are two major mechanisms of hydrogen formation – oxidation of zirconium and radiolysis of water [11]. For different types of nuclear power plants in structural materials accumulated various levels of the hydrogen atoms (from a few to thousands appm) [12]. Therefore, to study the hydrogen implantation effect on the properties of nitride-containing coatings is an urgent problem.

Previously we have investigated the implanted deuterium dose influence on the hardness and structure of TiN [13], TiAlSiN, TiAlYN [14] coatings and high-entropy TiZrNbHfVN [15] coating. It has been established that the deuterium thermodesorption spectrum (TDS) structure is a function of the implanted deuterium dose. As the implanted deuterium dose increases the temperature range of deuterium desorption from the coatings extends towards the temperature decrease [13, 14]. When the irradiation dose exceeds  $5 \cdot 10^{17}$  D/cm<sup>2</sup> the hardness of nitride coatings becomes almost twice as little [15].

Among two-component nitride coatings the CrN coating demonstrates the highest corrosion resistance in the super-critical water [16]. Application of the CrN coating, as one of the protective layers in zirconium fuel element tubes, sharply increases their resistance to the high-temperature air oxidation [17–19]. However, there are no sufficient data available as to the behavior of this coating under irradiation. For example, in [20] it is shown that the CrN corrosion resistance in the super-critical water can be decreased under  $\gamma$ -irradiation. The authors of [21] have observed the change in the lattice parameters, microstresses and grain size of the magnetron CrN coatings deposited on the silicon substrate under irradiation with 120 keV Ar ions at a dose of  $1 \cdot 10^{16}$  ions/cm<sup>2</sup>. The structure stability after irradiation of nanocrystalline CrN coatings was studied in [22]. It has been established that under nitrogen ion irradiation to the damage levels of 25 dpa their electrical resistivity increases. At the same time, the radiation exposure does not exert significant influence on the coating grain size and does not lead to their amorphization.

In the literature data on the changes of the mechanical properties of CrN coating after irradiation are absent. For use protective coating in the hydrogen (deuterium) containing environment it will need to determine what concentration of accumulated deuterium can cause structural changes and degradation of the mechanical properties of the coatings.

In this paper we investigate the implanted deuterium dose influence on the mechanical properties, structure, morphology and temperature ranges of deuterium desorption from CrN coatings prepared by a vacuum-arc deposition.

### 1. EXPERIMENTAL

Coatings with 5  $\mu$ m thickness were deposited from the vacuum-arc plasma stream [23] separated from macroparticles under 0.36 Pa nitrogen pressure, 100 A arc current and -100 V bias potential on the polished ( $R_a \sim 20$  nm) substrates made from Ch18Ni10T steel (20 $\times$ 10 $\times$ 1.5 mm). Temperature of specimens during

deposition did not exceed 700 K. Cathodes ( $\varnothing$  60 mm) were of chromium (99.9%).

The coatings were irradiated with a 24 keV  $D_2^+$  ion beam at doses from  $5 \cdot 10^{16}$  to  $1.5 \cdot 10^{18}$  D/cm<sup>2</sup> at temperature of 293 K. The temperature range of ion-implanted deuterium desorption from the specimens was investigated by the thermodesorption spectroscopy method using the device “Skif” [24]. The specimens were placed on the heaters made of Cr18Ni10T steel ribbon. The temperature was measured with a tungsten-rhenium thermocouple VR5/20 attached to the specimen. After implantation of a given deuterium dose the beam was stopped and then the heating was switched on. During heating the specimen temperature was increasing to  $\sim 1600$  K by the linear law versus time with an average heating rate of  $\sim 3.5$  K/s. Deuterium release in the measuring chamber was recorded with a mass-spectrometer by  $m = 4$  a.m.u. ( $D_2^+$ ). The implanted deuterium distribution profile was calculated by the program SRIM 2008 [25]. Calculation results are shown in Fig. 1. Maximum of deuterium profile is at a depth of  $\sim 104$  nm, and the maximum depth of the implanted layer is about 250 nm. We have previously shown that the calculated depth of deuterium is in good agreement with the measured in CrN coatings [26].

The phase composition and substructure of coatings were investigated by the method of X-ray diffraction analysis with a diffractometer DRON-4-07 in the filtered copper anode radiation (Cu-K $\alpha$  radiation). Diffraction patterns were taken by the  $\theta$ -2 $\theta$  scanning circuit with a Bragg-Brentano focusing within the angle intervals from 25 to 100 degrees. The diffraction pattern processing was performed using the computer program New\_Profile. By the position of diffraction lines identified as lines of nitride with a cubic structure of NaCl type the crystalline lattice period in the normal-to-film surface direction ( $a$ ) was determined. The crystallite size in the nitride coating was evaluated by the broadening of line (200) (L) from the Scherrer relation.

The surface morphology of the coatings before and after irradiation was inspected with a scanning atomic-force microscope (AFM) NanoScope IIIa in the periodic contact mode. Silicon probes having a nominal point radius of 10 nm were used.

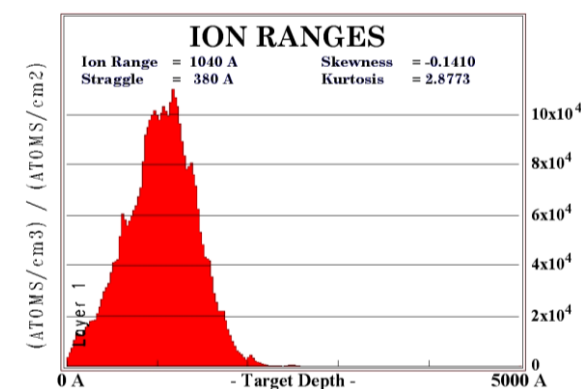


Fig. 1. The depth distribution profile of the ion-implanted deuterium with an energy of 24 keV in the CrN coating (calculated by SRIM 2008)

Nanoindentation was performed by means of the instrument Nanoindenter G200 (“Agilent Technologies”, USA) using a Berkovich diamond indenter having a 230 nm radius. The instrument is provided with an attachment designed for continuous control of the contact stiffness (CSM) that makes it possible to determine the dependence of the hardness and elastic modulus on the indenter penetration depth from the results of a single test. The hardness was measured to the indenter penetration depth of 300 nm. The tests were conducted with a constant deformation rate in an imprint equals to  $0.05$  s<sup>-1</sup>. The hardness and the elastic modulus were determined by the method of Oliver and Pharr [27].

## 2. RESULTS AND DISCUSSION

Fig. 2 presents the diffraction pattern of the as-deposited CrN coating. Here besides the substrate lines (denoted by S) one can see the lines of CrN nitride having a cubic structure (NaCl-type structure). The dashed lines show the CrN peak position (PDF card number No 11-0065, JCPDS cards numbers: 03-065-6914; 03-065-9001; 03-065-2829). The observed nitride line shift on the diffraction patterns towards the smaller angles, relatively to the position of corresponding nitride lines, can be caused by formation of compression residual stresses in coatings.

On the diffraction pattern of CrN coatings only lines (200) and (311) are visible. The crystallite size of the coating is 11 nm, the lattice parameter is  $a = 0.424$  nm. A low intensity of lines, a high level and characteristic shape of the background suggests that the CrN coating contains, besides crystalline nitride, a significant amount of X-ray amorphous phase.

The deuterium ion implantation at a dose of  $1.5 \cdot 10^{18}$  D/cm<sup>2</sup> does not lead to significant changes in the diffraction patterns of coatings: the pattern looks unchanged, new diffraction reflections do not appear, the width of lines and their intensity relation show no changes that evidence on the coating structure stability. The absence of changes on the CrN coating diffraction pattern can be explained by the fact that deuterium interacts mainly with the amorphous component of this condensate, and its implantation depth is insufficient for the X-ray diffraction analysis.

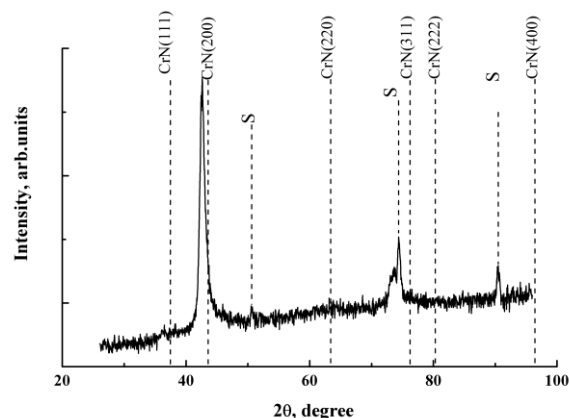


Fig. 2. Diffraction pattern of the CrN coating

The AFM images of the surface fragments of unirradiated and irradiated coatings are shown in Fig. 3,a,b. The relief of as-deposited films has a cellular structure which is characteristic for the method applied. The roughness is  $\sim 60$  nm. Deuterium implantation at a dose of  $1.5 \cdot 10^{18}$  D/cm<sup>2</sup> significantly changes the coating surface that can be interpreted as a blister formation.

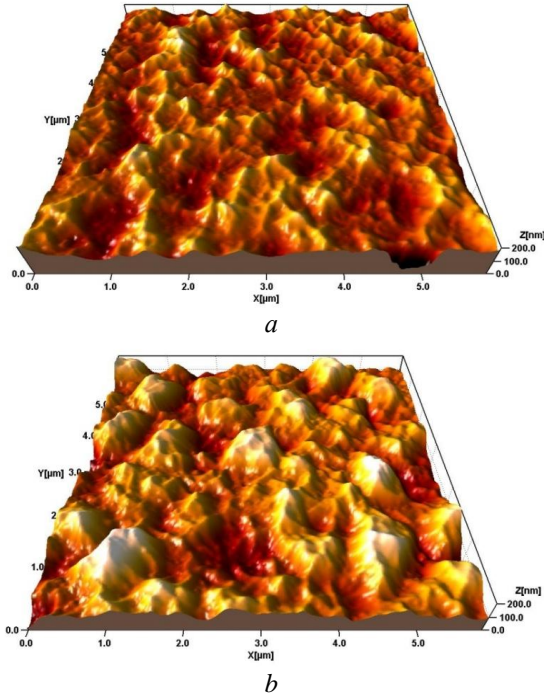


Fig. 3. Morphology of the CrN coating surface before (a) and after (b) deuterium implantation at a dose of  $1.5 \cdot 10^{18}$  D/cm<sup>2</sup>

One can see (see Fig. 3,b) that on the CrN coating an intensive increase of cellular sizes takes place. Blisters cover  $\sim 30\%$  of the surface, their height is  $\sim 50 \dots 200$  nm and the characteristic volume of a single blister is  $\sim 1 \cdot 10^8$  nm<sup>3</sup>. As a result of blister formation the coating surface roughness increases to  $R_a \approx 200$  nm.

The authors of [28] have observed the hydrogen blistering on the specimens of TiN and HfN nitride coatings irradiated with 40 keV deuterium ions at a dose of  $1.25 \cdot 10^{18}$  D/cm<sup>2</sup>. It should be noted that in our case blisters do not break up even at a maximum irradiation dose of  $1.5 \cdot 10^{18}$  D/cm<sup>2</sup> probably due to the presence in the CrN coatings structure of an amorphous component which promotes the deuterium dissolution in the implantation layer.

Fig. 4 presents the values of the hardness and elastic modulus for coatings before irradiation and after deuterium irradiation at doses within the range  $5 \cdot 10^{16} \dots 1.5 \cdot 10^{18}$  D/cm<sup>2</sup> at a depth of indenter penetration to 300 nm. It is seen that the CrN coatings are characterized by the high hardness of  $\sim 30$  GPa and the elastic modulus of  $\sim 330$  GPa. As a result of deuterium ion implantation the hardness and elastic modulus of the CrN coating are decreased. The implantation dose range can be conventionally divided into three parts by the degree of their influence on the mechanical properties of the coating. The changes are minimal at a dose of  $5 \cdot 10^{16}$  D/cm<sup>2</sup>, and at doses of  $(1 \dots 5) \cdot 10^{17}$  D/cm<sup>2</sup> the

hardness decreases insignificantly (by 10...15%). A sharp decrease of the nanohardness to  $\sim 12$  GPa and of the elastic modulus to 200 GPa occurs under deuterium irradiation at doses of  $(1 \dots 1.5) \cdot 10^{18}$  D/cm<sup>2</sup>.

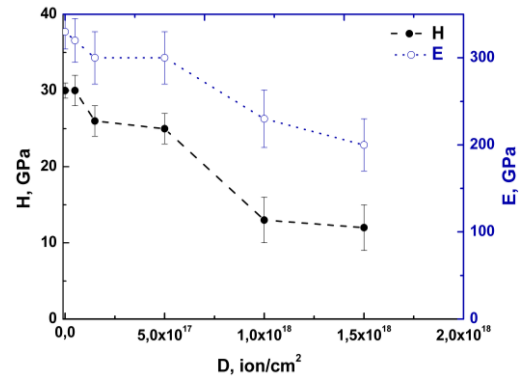


Fig. 4. Effect of the deuterium irradiation dose on the hardness (H) and elastic modulus (E) of CrN coatings

The indenter penetration diagrams obtained for the as-deposited CrN coatings and for the coatings irradiated at a dose of  $1.5 \cdot 10^{18}$  D/cm<sup>2</sup> are presented in Fig. 5. For the as-deposited CrN coating the penetration diagram is typical, i. e. the indenter tip moves with load increasing. After coating irradiation the character of the load-displacement curves varies. For all the indentations on the load-displacement curve a sharp increase of the indenter movement by 10...25 nm (pop-in) is observed and the depth of pop-in formation for each indentation is different (200...250 nm) (see Fig. 5). This is somewhat deeper than the calculated profile maximum of deuterium depth of  $\sim 160$  nm. The critical load value, at which a pop-in is formed, varies between 20 and 25 mN. In our opinion such a behavior of the penetration diagram for CrN coatings irradiated at a dose of  $1.5 \cdot 10^{18}$  D/cm<sup>2</sup> can be explained by the presence in the coating of regions with very low hardness. It is quite possible that the regions being formed are hydride blisters. The authors of [6] have observed a similar effect of the pop-in formation under irradiation of Ti-Zr-N magnetron coatings with 360 keV Xe ions at a dose of  $8 \cdot 10^{14}$  ions/cm<sup>2</sup> that explained by the formation of voids and gas bubbles in the coating. Judging from a sharp decrease of the nanohardness in Fig. 3, the blister formation begins after the implantation dose above  $5 \cdot 10^{17}$  D/cm<sup>2</sup>.

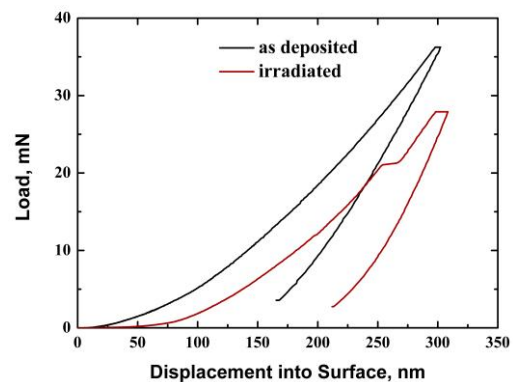


Fig. 5. Load-displacement curves of the CrN coating: as-deposited and irradiated at a dose of  $1.5 \cdot 10^{18}$  D/cm<sup>2</sup>

So, the presence of pop-ins in the loading diagram for the irradiated coating compared with the unirradiated coating confirms the assumption of blistering formation in the CrN coatings irradiated at a dose of  $1.5 \cdot 10^{18} \text{ D/cm}^2$ .

Fig. 6 shows the deuterium thermodesorption spectra of CrN coatings irradiated at different doses.

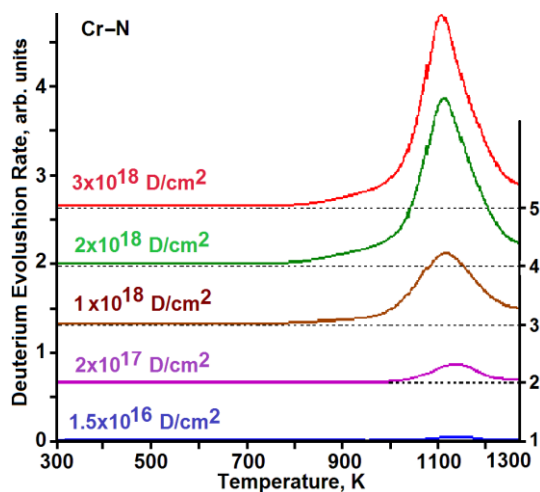


Fig. 6. Deuterium thermodesorption spectra of CrN coatings irradiated at different doses:  $1.5 \cdot 10^{16} \dots 3 \cdot 10^{18} \text{ D/cm}^2$

One can see that in the deuterium TDS of CrN coatings there is only a single desorption temperature range with the center of gravity at 1120 K throughout the range of implantation doses under consideration. A single-peaked behavior of the deuterium TDS points to the presence of only one coating structure state which is unchangeable throughout the range of implanted deuterium.

Fig. 7 presents the dependence of the total amount of retained deuterium on the irradiation dose. This dependence is linear only up to a dose of  $2.5 \cdot 10^{18} \text{ D/cm}^2$ . Then a sharp deviation from the linearity and the attainment of saturation is observed.

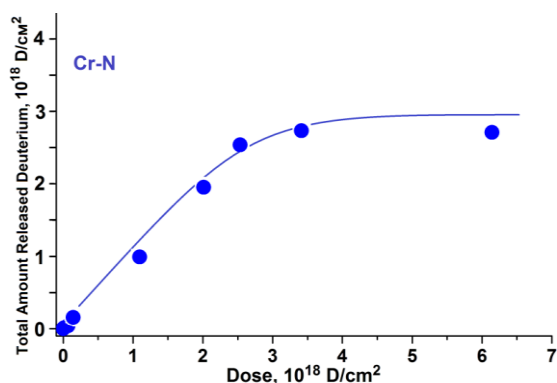


Fig. 7. Total amount of desorbed deuterium as a function of an irradiation dose in the CrN coating

Implanted deuterium in the CrN coating is practically motionless and takes place within the bounds of the implantation profile. Therefore, taking into account the average projective range of  $24 \text{ keV D}_2^+$  ions in the chromium nitride it is easy to show that at a saturation dose of  $2.5 \cdot 10^{18} \text{ D/cm}^2$  the deuterium

concentration in the implantation layer is of about 2 D atoms per 1 Cr atom. A single peak in the deuterium TDS generally characterizes the formation and decomposition of the deuterium solid solution phase in metals [29] (CrN coating in our case). A lack of low-temperature peak formation in the thermodesorption spectra by increasing the implanted deuterium dose, characteristic for hydride-forming metals, indicates to the absence of deuterium-CrN coating interaction leading to the formation of hydrides with low-temperature decomposition.

## CONCLUSIONS

1. A CrN coating, deposited from the filtered vacuum-arc plasma stream, has a cubic crystalline structure with an axial texture and crystallite size  $\approx 11 \text{ nm}$ . The methods of X-ray diffraction analysis did not reveal a new phase formation at a deuterium irradiation dose of  $\sim 1.5 \cdot 10^{18} \text{ D/cm}^2$ .

2. The atomic-force microscopy data show that deuterium irradiation up to a dose of  $\geq 1 \cdot 10^{18} \text{ D/cm}^2$  causes the formation on the coating surface of blisters having a characteristic height of  $\sim 150 \dots 200 \text{ nm}$  which cover about 30% of the irradiated coating surface.

3. A CrN coating is characterized by a high hardness of  $\sim 30 \text{ GPa}$ . The deuterium ion implantation results in the hardness decrease. In the range of doses from  $5 \cdot 10^{16}$  to  $5 \cdot 10^{17} \text{ D/cm}^2$  the hardness decreases by 10...15%. The nanohardness decrease to  $\sim 50\%$  occurs at doses  $> 5 \cdot 10^{17} \text{ D/cm}^2$ , most likely, due to the blister formation.

4. A maximum deuterium concentration in the implantation layer of the CrN coating is  $\sim 2 \text{ D atoms per 1 Cr atom}$  after irradiation at a dose of  $\sim 2.5 \cdot 10^{18} \text{ D/cm}^2$ .

5. In the deuterium desorption spectrum of CrN coatings only a single temperature peak at temperature of 1120 K is observed throughout the range of implanted doses being investigated that indicates to a lack of hydride formation.

The obtained investigation results show that significant changes in the CrN coatings deposited by the vacuum-arc method take place at implanted deuterium doses of  $> 5 \cdot 10^{17} \text{ D/cm}^2$ .

## ACKNOWLEDGMENTS

We are also thankful to Dr. P.M. Lytvyn for carrying out atomic force microscopy tests at the V.E. Lashkarev Institute of Semiconductor Physic, NAS of Ukraine, Kiev.

## REFERENCES

- I.I. Aksenov, A.A. Andreev, V.A. Belous, V.E. Strel'nitskij, V.M. Khoroshikh. *Vacuum-Arc Plasma sources, coatings deposition, surface modification*. Kyiv: "Naukova dumka", 2012, 728 p.
- R. Bès, C. Gaillard, N. Millard-Pinard, S. Garvarini, P. Martin, S. Cardinal, C. Esnouf, A. Malchère, A. Perrat-Mabilon. Xenon behavior in TiN: A coupled XAS/TEM study // *Journal of Nuclear Materials*. 2013, v. 434, p. 56-64.
- L. Jiao, A. Chen, M.T. Myers, M.J. General, L. Shao, X. Zhang, H. Wang. Enhanced ion irradiation

- tolerance properties in TiN/MgO nanolayer films // *Journal of Nuclear Materials*. 2013, v. 434, p. 217-222.
4. H. Wang, R. Araujo, J.G. Swadener, Y.Q. Wang, X. Zhang, E.G. Fu, T. Cagin. Ion irradiation effects in nanocrystalline TiN coatings // *Nuclear Instruments and Methods in Physics Research B*. 2007, v. 261, p. 1162-1166.
  5. M. Popović, M. Novaković, N. Bibić. Structural characterization of TiN coatings on Si substrates irradiated with Ar ions // *Materials Characterization*. 2009, v. 60, p. 1463-1470.
  6. V.V. Uglov, D.P. Rusalski, S.V. Zlotski, A.V. Sevriuk, G. Abadias, S.B. Kislitsin, K.K. Kadyrzhayev, I.D. Gorlachev, S.N. Dub. Stability of Ti-Zr-N coatings under Xe-ion irradiation // *Surface and Coatings Technology*. 2010, v. 204, p. 2095-2098.
  7. M. Kawaia, H. Kokawa, M. Michiuchi, et al. Present status of study on development of materials resistant to radiation and beam impact // *Journal of Nuclear Materials*. 2008, v. 377, p. 21-27.
  8. A.A. Andreev, V.N. Voevodin, O.V. Sobol', et al. Regularities in the effect of model ion irradiation on the structure and properties of vacuum-arc nitride coatings // *Problems of Atomic Science and Technology*. 2013, N 5(87), p. 142-146
  9. M.I. Guseva, Yu.V. Martynenko. Radiation blistering // *Uspekhi Fizicheskikh Nauk*. 1981, v. 135, N 4, p. 671-691 (in Russian).
  10. T. Laursen, M. Leger, Xin-Pei Ma, et al. The measurement of the deuterium concentration distributions in deuteride blisters on zirconium-alloy pressure tube material // *Journal of Nuclear Materials*. 1989, N 165, p. 156-163.
  11. X. Hu, K.A. Terrani, B.D. Wirth. Hydrogen desorption kinetics from zirconium hydride and zirconium metal in vacuum // *Journal of Nuclear Materials*. 2014, v. 448, p. 87-95.
  12. F.A. Garner, E.P. Simonen, B.M. Oliver, L.R. Greenwood, M.L. Grossbeck, W.G. Wolfer, P.M. Scott. Retention of hydrogen in fcc metals irradiated at temperatures leading to high densities of bubbles or voids // *Journal of Nuclear Materials*. 2006, v. 356, p. 122-135.
  13. A.S. Kuprin, O.M. Morozov, V.D. Ovcharenko, et al. Nanocrystalline TiN films after deuterium ions irradiation // *International conference Functional materials and nanotechnologies*, Tartu, Estonia in April, 21-24, 2013, PO-170.
  14. V.A. Belous, A.S. Kuprin, N.S. Lomino, et al. Influence of Deuterium Ion Implantation on the Structure and Hardness of Nanocrystalline Films // *Proceedings of the 2-nd International Conference Nanomaterials: Applications and Properties*, Alushta, Ukraine, 17-22, September, 2012, v. 1, N 4, 04RES07 (3 p.).
  15. A.S. Kuprin, O.M. Morozov, V.A. Belous et al. Effects of Deuterium Implantation Dose on Hardness and Deuterium Desorption Temperature Range from High-Entropy TiVZrNbHf and TiVZrNbHfN Coatings // *Proceedings of the International Conference on Nanomaterials: Applications and Properties*. 2013, v. 2, N 2, 02FNC20 (3 p.).
  16. S. Korablov, M.A.M. Ibrahim, M. Yoshimura. Hydrothermal corrosion of TiAlN and CrN PVD films on stainless steel // *Corrosion Science*. 2005, v. 47, p. 1839-1854.
  17. A.S. Kuprin, V.A. Belous, V.N. Voevodin, et al. High-temperature air oxidation of E110 and Zr-1Nb alloy claddings with coatings // *Problems of Atomic Science and Technology*. 2014, N 1 (89), p. 126-132.
  18. A.S. Kuprin, V.A. Belous, V.N. Voevodin et al. Vacuum-arc chromium-based coatings for protection of zirconium alloys from the high-temperature oxidation in air // *Journal of Nuclear Materials*. 2015, v. 465, p.400-406.
  19. K. Daub, R. Van Nieuwenhove, H. Nordin. Investigation of the impact of coatings on corrosion and hydrogen uptake of Zircaloy-4 // *Journal of Nuclear Materials*. 2015, v. 467, p.260-270.
  20. Kawana, H. Ichimura, Y. Iwata, S. Ono. Development of PVD ceramic coatings for valve seats // *Surface and Coatings Technology*. 1996, v. 86-87, p. 212-217.
  21. M. Novaković, M. Popović, N. Bibić. Ion-beam irradiation effects on reactively sputtered CrN thin films // *Nuclear Instruments and Methods in Physics Research B*. 2010, v. 268, p. 2883-2887.
  22. A. Guglya, I. Neklyudov, R. Vasilenko. Effect of helium ion irradiation on the structure and electrical resistivity of nanocrystalline CrN and V-N coatings // *Radiation Effects and Defects in Solids*. 2007, v. 162, issue 9, p. 643-649.
  23. I.I. Aksenov, V.M. Khoroshikh. Filtering shields in vacuum-arc plasma sources // *Materials Science Forum*. 1998, v. 287-288, p. 283-286.
  24. V.V. Ruzhitsky, Yu.A. Gribanov, V.F. Rybalko, S.M. Khazan, A.N. Morozov, I.S. Martynov // *Voprosy Atomnoj Nauki I Tekhniki. Serya "FRP RM"*. 1989, issue 4(51), p. 84-89 (in Russian).
  25. <http://www.srim.org/>
  26. G.D. Tolstolutskaia, I.E. Kopanetz, V.V. Ruzhitskiy, V.A. Bilous, A.S. Kuprin, V.D. Ovcharenko, R.L. Vasilenko, S.A. Leonov. Decrease of hydrogen saturation of zirconium alloys at modification of surface by complex ion-plasma treatment // *Problems of Atomic Science and Technology*. 2015, N 2 (96), p. 119-123.
  27. W. Oliver, G. Pharr. Measurement of hardness and elastic modulus by instrumented indentation: Advances in understanding and refinements to methodology // *J. Mater. Res*. 2004, v. 19, N 1, p. 3-20.
  28. R.G. Duckworth, I.H. Wilson. Ion bombardment of group IV elemental metal and synthetic nitride films // *Thin Solid Films*. 1979, v. 63, issue 2, 1 November, p. 289-297.
  29. I.M. Neklyudov, O.M. Morozov, V.G. Kulish, V.I. Zhurba. P.A. Khaimovich, A.G. Galitskiy. Hydrogen diagnostics of structural states in 18Cr10NiTi steel // *Journal of Hydrogen Energy*. 2011, v. 36, p. 1192-1195.

## **ВЛИЯНИЕ ДОЗЫ ИМПЛАНТИРОВАННОГО ДЕЙТЕРИЯ НА СВОЙСТВА ПОКРЫТИЙ CrN**

*А.С. Куприн, В.А. Белоус, А.Н. Морозов, В.Д. Овчаренко, С.Н. Дуб, Г.Н. Толмачева,  
Е.Н. Решетняк, В.И. Журба, В.О. Проколаева*

Методами рентгеноструктурного анализа, атомно-силовой микроскопии, наноиндентирования и термодесорбционной спектроскопии исследовано влияния дозы ( $5 \cdot 10^{16} \dots 1,5 \cdot 10^{18} \text{ D/cm}^2$ ) имплантированного дейтерия с энергией 24 кэВ на структуру, морфологию поверхности и механические свойства вакуумно-дуговых покрытий CrN. Имплантированный дейтерий в интервале доз  $5 \cdot 10^{16} \dots 5 \cdot 10^{17} \text{ D/cm}^2$  приводит к уменьшению на 10...15% нанотвердости и модуля упругости покрытий. Облучение дозами  $\geq 1 \cdot 10^{18} \text{ D/cm}^2$  вызывает резкое снижение нанотвердости покрытий из-за формирования блистеров, которые занимают около 30% поверхности покрытия CrN. Имплантация дейтерия не приводит к образованию новых фаз в покрытии CrN.

## **ВПЛИВ ДОЗИ ІМПЛАНТОВАНОГО ДЕЙТЕРІЮ НА ВЛАСТИВОСТІ ПОКРИТТІВ CrN**

*О.С. Купрін, В.А. Білоус, О.М. Морозов, В.Д. Овчаренко, С.М. Дуб, Г.М. Толмачова,  
О.М. Решетняк, В.І. Журба, В.О. Проколаєва*

Методами рентгеноструктурного аналізу, атомно-силової мікроскопії, наноіндентування і термодесорбційної спектроскопії досліджено вплив дози ( $5 \cdot 10^{16} \dots 1,5 \cdot 10^{18} \text{ D/cm}^2$ ) імпантованого дейтерію з енергією 24 кеВ на структуру, морфологію поверхні та механічні властивості вакуумно-дугових покриттів CrN. Імпантований дейтерій в інтервалі доз  $5 \cdot 10^{16} \dots 1,5 \cdot 10^{17} \text{ D/cm}^2$  призводить до зменшення на 10...15% нанотвердості і модуля пружності покриттів. Опромінення дозами  $\geq 1 \cdot 10^{18} \text{ D/cm}^2$  викликає різке зниження нанотвердості покриттів через формування блистерів, які займають близько 30% поверхні покриття CrN. Імпантация дейтерію не призводить до утворення нових фаз у покритті CrN.